Materials Letters 324 (2022) 132817

Contents lists available at ScienceDirect

Materials Letters

journal homepage: www.elsevier.com/locate/matlet

Investigation of the orientation dependence of marforming on superelasticity and shape memory effect in equiatomic TiNi single crystals under compression

I.V. Kireeva *, Y.I. Chumlyakov, A.V. Vyrodova, Z.V. Pobedennaya, E.S. Marchenko

National Research Tomsk State University, Tomsk 634050, Russian Federation

ARTICLE INFO

Keywords:
Equiatomic $Ti_{50}Ni_{50}$ single crystals
Shape memory effect
Superelasticity
$[001]_{B2}$ orientation
Compression strain

ABSTRACT

The shape memory effect (SME) and superelasticity (SE) after marforming (deformation in the martensitic phase at 203 K, followed by annealing at 713 K, 0.5 h) were studied in the equiatomic TiNi crystals under compression. Marforming was carried out along $[001]_{B2}$ and $[011]_{B2}$ directions of B2-phase after strain of $\varepsilon = 1.5\varepsilon_0$ (ε_0 is the lattice deformation, which depends on the crystal orientation). SME and SE after marforming were studied along $[001]_{B2}$ direction. It was shown that the maximum stress level of B2-phase $\sigma_{cr}(B2) = 750$ MPa, the lowest values of mechanical $\Delta\sigma = 100$ MPa and thermal $\Delta T_h = 32$ K hysteresis and the maximum temperature range of SE $\Delta T_{SE} = 77$ K were observed when marforming under compression was realized along the $[001]_{B2}$ direction.

1. Introduction

Equiatomic TiNi shape memory alloy (SME) undergoing single-stage B2-B19' martensitic transformation (MT) is characterized by good ductility, fatigue and corrosion resistance and biocompatibility required for applications in medicine and other fields [1,2]. However, the equiatomic TiNi alloy is not used in the quenched state because of the low strength properties of the high-temperature B2-phase and the absence of superelasticity (SE) [1,2]. The necessary conditions for SE in single- and polycrystals of equiatomic and near equiatomic TiNi composition were obtained as a result of thermomechanical treatments, namely, marforming (deformation in the martensite phase, followed by annealing) and ausforming (deformation in the high-temperature B2-phase, followed by annealing) [3,4].

In the present paper, in the equiatomic TiNi crystals, the problem was posed, firstly, to obtain SE after marforming under compression and, secondly, to study the dependence of marforming on the crystallographic direction. To achieve this goal, the samples had the compression axis $[001]_{B2}$ and the orientation of the side faces $\{011\}_{B2}$. In the martensitic state, one part of the samples was deformed along the $[001]_{B2}$ direction and the other in the $[011]_{B2}$ direction by $\varepsilon = 1.5\varepsilon_0$ (ε_0 is the lattice deformation, which depends on the crystal orientation [1,2,5]), exceeding the theoretical value of ε_0 for B2-B19′ MT, for the corresponding orientation. The SE and SME after marforming along different crystallographic directions were studied along the $[001]_{B2}$ compression axis. The choice of the $[001]_{B2}$ compression axis and the $\{011\}_{B2}$ orientation of the side faces of the samples was determined, firstly, by the close value of ε_0 for the B2-B19' MT under compression ($\varepsilon_0 = 4.5\%$ in the $[001]_{B2}$ orientation and $\varepsilon_0 = 5.15\%$ in the $[011]_{B2}$ orientation [5]) and, secondly, different stress levels of the high-temperature B2-phase due to different Schmid factor for slip along a $\langle 100\rangle\{110\}_{B2}$ system in the B2-phase ($m_{sl} = 0$ in the $[001]_{B2}$ orientation and $m_{sl} = 0.35$ in the $[011]_{B2}$ orientation [6]).

2. Experiments

Single crystals of the equiatomic TiNi (at%) alloy were grown by the Bridgman method in graphite crucibles and helium atmosphere. Compressive specimens with a size of $4 \times 4 \times 8$ mm^3 were cut using wire electrical discharge machining. Samples were homogenized at 1253 K for 2 h, in a helium atmosphere, followed by water quenching at 296 K. Start M_s, R_s, M_s^1 and M_s^2 and finish M_f temperatures of the forward MTs during cooling and start A_s and finish A_f temperatures of the reverse MT during heating, were obtained by differential scanning calorimetry (DSC) (NETZSCH DSC 404F1 machine with a cooling/heating rate of 10 K/min). Critical stresses and SE were investigated on an Instron 5969 testing machine at deformation rate of 4×10^{-4} s^{-1}. SME was studied on home-made dilatometer during cooling and heating in the temperature

* Corresponding author.
E-mail address: kireeva@spti.tsu.ru (I.V. Kireeva).

https://doi.org/10.1016/j.matlet.2022.132817
Received 27 May 2022; Received in revised form 5 July 2022; Accepted 7 July 2022
Available online 11 July 2022
0167-577X/© 2022 Elsevier B.V. All rights reserved.

range from 77 to 400 K, at a constant stress in the cycle, with a heating/cooling rate of 10 K/min. The crystal structure was investigated using a JEOL-2010 transmission electron microscope (TEM) at an accelerating voltage of 200 kV. Marforming included deformation $\varepsilon = 1.5\varepsilon_0$ in the martensitic phase at 203 K ($\varepsilon = 6.75\%$ for $[001]_{B2}$ orientation and $\varepsilon = 7.72\%$ for $[011]_{B2}$ orientation), followed by annealing at 713 K, 0.5 h. After annealing at T = 713 K, 0.5 h, residual deformation of 1–1.5% was observed in the samples. SE and SME were studied after quenching (Crystals I); after marforming along the $[001]_{B2}$ compression axis (Crystals II) and after marforming along $[011]_{B2}$ orientation of the side face (Crystals III).

3. Results and discussion

TEM studies of the residual deformation after marforming revealed retained B19'-martensite with $(0\bar{2}1)_{Tw}$ twins in Crystals II (Fig. 1a) and with $(001)_{Tw}$ twins in Crystals III (Fig. 1b).These twins are not a solution of the phenomenological theory, describing the B2-B19' MT, but are mechanical twins that arise during low-temperature plastic deformation of B19'-martensite [1,2,4]. The R-phase in Crystals II and III was found near dislocations (Fig. 1c). In addition, a higher dislocation density was observed in Crystals III than in Crystals II.

In Crystals I, a one-stage B2-B19' MT was realized with a thermal hysteresis of $\Delta T_h = A_f–M_s = 33$ K. The DSC curves, upon cooling and heating, were found to exhibit one peak of exothermic and endothermic heat, which was associated with B2-B19′ and B19′-B2 MT, respectively (Fig. 1d). After marforming, the MT changed from a one-stage in Crystals I to a two-stage B2-R-B19' MT in Crystals II and III, which developed in a wider temperature range (Fig. 1e and f). On cooling, two sharp peaks and one diffuse peak were observed on the DSC curves. The first two peaks were associated with B2-R MT and R-B19' MT, respectively, in regions with a high dislocation density and with retained B19'-martensite, and the third peak was associated with B2-B19' MT in defect-free regions [4]. Upon heating, the MT peaks were not separated, and one peak of endothermic heat of B19'-R-B2 MT was observed (Fig. 1e and f). In Crystals III, the temperature M_s^1 for the R-B19' MT turned out to be higher by 11 K than in Crystals II, which may be due to the difference in the defect structure and requires additional studies.

In Crystals I, SE $\varepsilon_{SE} = 0.5\%$ was observed in a narrow temperature range $\Delta T_{SE} = 20$ K (Fig. 2a). SME under stress $\varepsilon_{SME} = 0.2\%$ appeared at $\sigma_{ex} = 50$ MPa and increased up to 2.8% at $\sigma_{ex} = 300$ MPa (Fig. 2b). The maximum value of $\varepsilon_{SME} = 2.8\%$ was less than the value of the lattice deformation $\varepsilon_0 = 4.5\%$ for B2-B19' MT in $[001]_{B2}$ orientation under compression. The dependence $\varepsilon_{tr}(T)$ was characterized by temperature hysteresis $\Delta T_h = A_f\text{-}M_s = 50$ K at $\sigma_{ex} = 250$ MPa (Fig. 2b).

After marforming, SE developed in a wider temperature range: in Crystals II, $\Delta T_{SE} = 77$ K and in Crystals III, $\Delta T_{SE} = 40$ K (Fig. 2c and e). It can be seen that in Crystals II $\sigma(\varepsilon)$ curve at superelastic strain of $\varepsilon_{SE} = 3–3.5\%$ was characterized by mechanical hysteresis $\Delta\sigma = 100$ MPa, which weakly depended on the test temperature. In Crystals III at $\varepsilon_{SE} = 3.5\%$, $\Delta\sigma = 200$ MPa at 313 K and decreased to 130 MPa at 343 K. The maximum SE value, established in experiments on cycling at one test temperature of 333 K, was 4.5% for Crystals II, which was equal to $\varepsilon_0 = 4.5\%$, and in the case of Crystals III, it was less than ε_0 and amounted to 3.8% (Fig. 2c and e, insert). SME in Crystals (II) and (III) appeared at stress $\sigma_{ex} = 12.5$ MPa (Fig. 2d and f). It is interesting to note that at the same level of $\sigma_{ex} < 150$ MPa in Crystals II, the SME value was greater than in Crystals III. At $\sigma_{ex} \geq 150$ MPa, the SME reached the maximum $\varepsilon_{SME} = 3.3\%$ in both Crystals (II) and (III), which was less than ε_{SE} and ε_0. At the same $\sigma_{ex} = 250$ MPa, ΔT_h on the $\varepsilon_{tr}(T)$ curves in Crystals II and III was 1.5 times less than in Crystals I and became equal to 32 and 35 K, respectively (Fig. 2b, d and f, insert).

The temperature dependence $\sigma_{cr}(T)$ for the three states turned out to be close (Fig. 3). Three stages were observed on the $\sigma_{cr}(T)$ dependence, which are characteristic of alloys undergoing the stress-induced MT [1,2]. The maximum in the $\sigma_{cr}(T)$ dependence corresponded to the M_d temperature, at which the $\sigma_{cr}(SIM)$ required for the stress-induced MT were equal to $\sigma_{cr}(B2)$ for the onset of plastic flow of the B2-phase. At $T < M_d$ up to the minimum stress σ_{min}, the $\sigma_{cr}(T)$ dependence exhibited a stage associated with the stress-induced MT, which was described by the

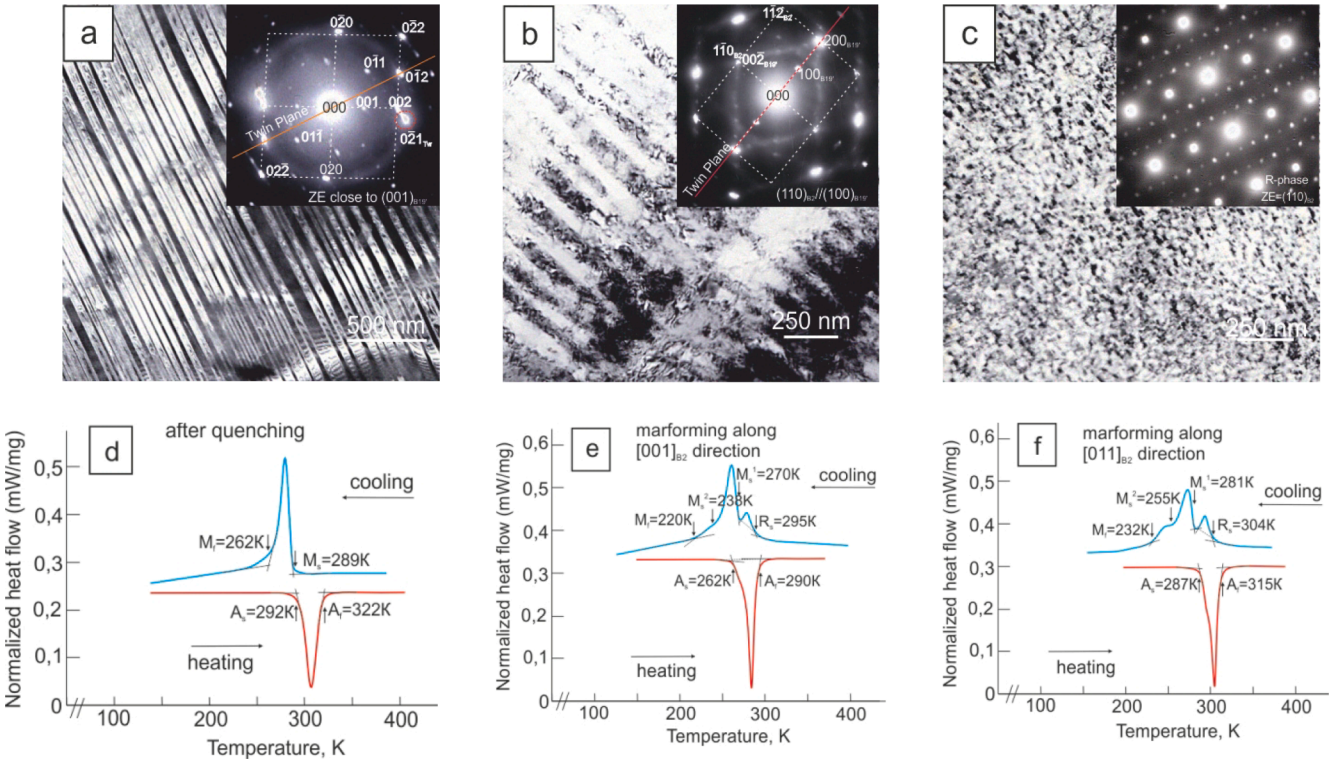

Fig. 1. Microstructure after marforming (a)-(c) and DSC curves (d)-(f) of the $[001]_{B2}$-oriented TiNi crystals.

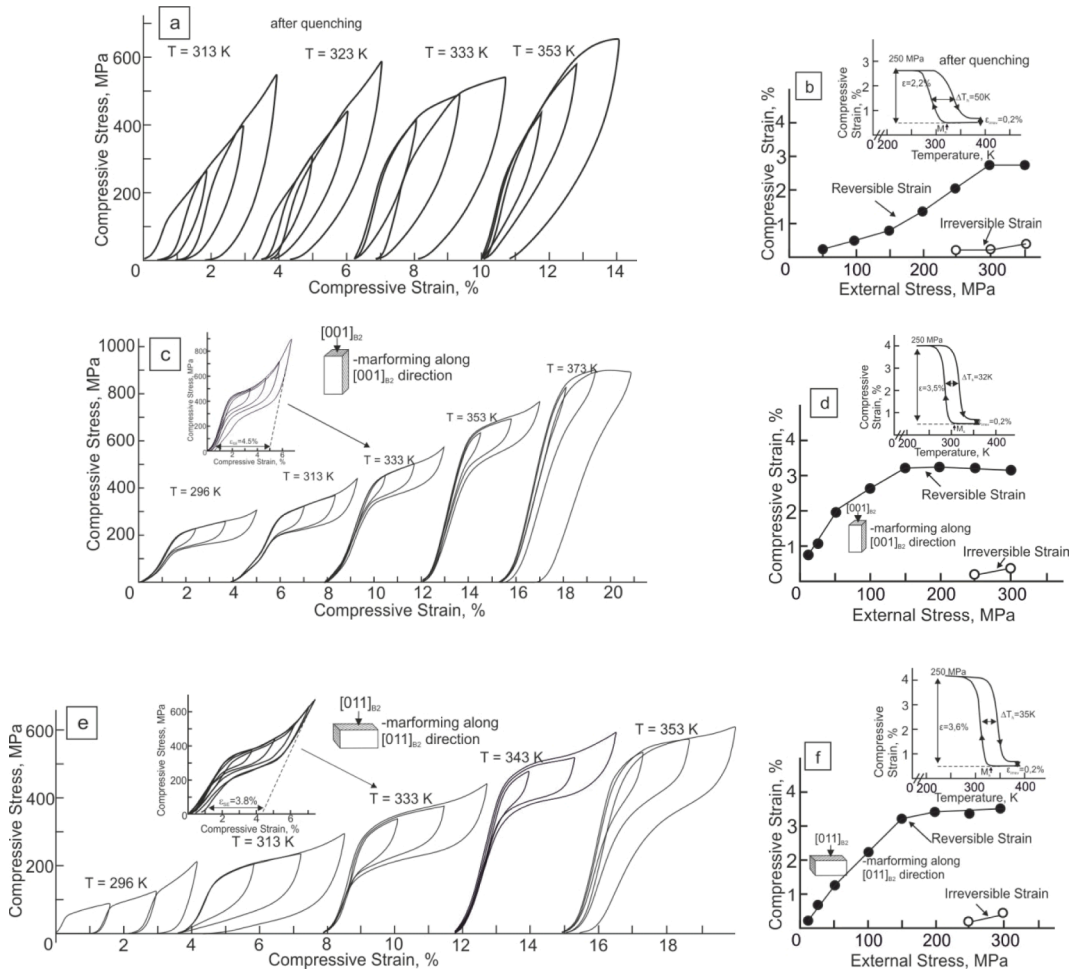

Fig. 2. Superelasticity and shape memory effect in the $[001]_{B2}$-oriented crystals of the equiatomic TiNi alloy under compression.

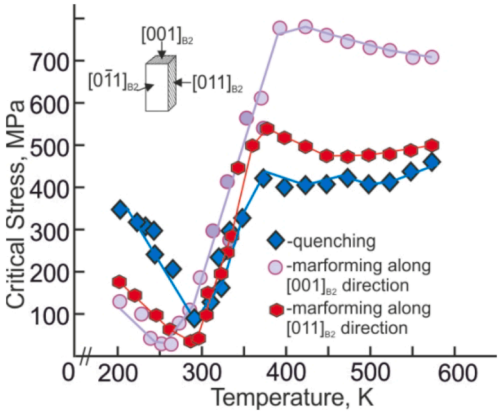

Fig. 3. Temperature dependence of the critical stresses of $[001]_{B2}$ equiatomic TiNi crystals under compression.

Clausius-Clapeyron relation [1,2]:

$$\frac{d\sigma_{cr}}{dT} = -\frac{\Delta H}{\varepsilon_0 T_0} = -\frac{\Delta S}{\varepsilon_0} \quad (1)$$

Here ΔH, ΔS is the change in enthalpy and entropy at MT, respectively, T_0 is the phase equilibrium temperature, and ε_0 is the lattice deformation. It can be seen that marforming along different crystallographic directions did not affect the $\alpha = d\sigma_{cr}(SIM)/dT$ (Fig. 3), which was explained by the close maximum ε_{SME} value for the three states (Fig. 2b, d and f) and followed from relation (1). The minimum on the $\sigma_{cr}(T)$ dependence was reached at $T = M_s$, which coincided with M_s for R-B19' determined from DSC curves (Fig. 1d–f). At $T < M_s$, the third stage was observed, associated with the reorientation of the cooling martensite. At $T > M_d$, the $\sigma_{cr}(T)$ dependence was determined by the temperature dependence of the B2-phase stresses, $\sigma_{cr}(B2)$. Marforming increased $\sigma_{cr}(B2)$ and lowered $\sigma_{cr}(M_s)$ in Crystals (II) and (III) as compared to Crystals I (Fig. 3). The decrease in $\sigma_{cr}(M_s)$ up to 30 and 50 MPa, respectively, in Crystals (II) and (III) was associated with: i) the development of a two-stage B2-R-B19' MT through the R-phase, which did not appear under stress due to the zero Schmid factor for B2-R MT, but lowered the barrier for the nucleation of B19'-martensite crystals under stress; ii) the facilitation of the B19'-martensite nucleation processes on defects [4]. As a result, after marforming, the plastic flow during the stress-induced MT in Crystals (II) and (III) became more difficult and ΔT_{SE} increased, while Δσ and ΔT_h decreased in comparison with Crystals I with lower properties of the B2-phase and high $\sigma_{cr}(M_s) = 120$ MPa.

According to the well-known phenomenological Otsuka-Wayman criterion [1,2], SE is manifested if the ratio of the strength properties of the high-temperature B2-phase $\sigma_{cr}(B2)$ to the stresses required for the martensite formation at the M_s temperature $\sigma_{cr}(M_s)$ is 4–5. In Crystals I with $\sigma_{cr}(B2) = 400$ MPa and $\sigma_{cr}(M_s) = 120$ MPa, the ratio $\sigma_{cr}(B2)/\sigma_{cr}(M_s) < 4$. The Otsuka-Wayman criterion for SE was not fulfilled and SE was practically not observed (Fig. 1a). As for the Crystals (II) and (III), the Otsuka-Wayman criterion for SE was satisfied, since at $\sigma_{cr}(B2)$ equal to 750 and 490 MPa and $\sigma_{cr}(M_s)$ equal to 30 and 50 MPa, respectively, the ratio $\sigma_{cr}(B2)/\sigma_{cr}(M_s)$ became 25 in Crystals (II) and 9.8

in Crystals (III). In Crystals (II), σ_{cr}(B2) was higher by 250 MPa than σ_{cr}(B2) in Crystals III (Fig. 3). This determined the higher ΔT_{SE} and lower $\Delta\sigma$ and ΔT_h values in Crystals II compared to Crystals III (Fig. 2c–f).

4. Conclusions

It has been found that in $[0\,0\,1]_{B2}$-oriented equiatomic TiNi crystals, the SE and its temperature range ΔT_{SE} under compression are controlled by the stress level of the high-temperature B2-phase after marforming. After marforming, the different stress level of B2-phase was due to the difference in the defect structure. The maximum $\sigma_{cr}(B2) = 750$ MPa, the lowest $\Delta\sigma = 100$ MPa and $\Delta T_h = 32$ K values, as well as the maximum $\Delta T_{SE} = 77$ K were observed when marforming under compression was realized along the $[0\,0\,1]_{B2}$ direction.

CRediT authorship contribution statement

I.V. Kireeva: Supervision, Conceptualization, Investigation, Writing – original draft, Writing – review & editing. **Y.I. Chumlyakov:** Conceptualization, Supervision. **A.V. Vyrodova:** Investigation. **Z.V. Pobedennaya:** Investigation. **E.S. Marchenko:** Project administration, Funding acquisition.

Declaration of Competing Interest

The authors declare that they have no known competing financial interests or personal relationships that could have appeared to influence the work reported in this paper.

Data availability

Data will be made available on request.

Acknowledgments

This work was supported by the Ministry of Education and Science of the Russian Federation, Project No. FSWM-2020-0022 and by the Tomsk State University Development Programme (Priority-2030).

References

[1] K. Otsuka, C.M. Wayman (Eds.), Shape Memory Materials, Cambridge Univ. Press, Cambridge, 1999.
[2] K. Otsuka, X. Ren, Prog. Mater. Sci. 50 (5) (2005) 135–678.
[3] E. Hornbogen, V. Mertinger, D. Wurzel, Scripta Mater. 44 (1) (2001) 171–178.
[4] Y.I. Chumlyakov, I.V. Kireeva, A.V. Vyrodova, A.A. Saraeva, Z.V. Pobedennaya, J. Alloys Compd. 896 (2021) 162841.
[5] H. Sehitoglu, R. Hamilton, D. Canadinc, X.Y. Zhang, K. Gall, I. Karaman, Y. Chumlyakov, H.J. Maier, Metall. Mater. Trans. A 34 (5) (2003) 5–13.
[6] H. Sehitoglu, I. Karaman, X. Zhang, A. Viswanath, Y. Chumlyakov, H.J. Maier, Acta Mater. 49 (17) (2001) 3621–3634.